

## Research Article

# Nanobiocomposite of fungal asparaginase and magnetic nanoparticle: Synthesis, Characterization and Anticancer Activity against MCF-7 and HT-29 Cancer cell lines

G. Baskar\*, Garrick Bikku George

Department of Biotechnology, St. Joseph's College of Engineering,  
Chennai – 600 119, India.

\*Corresponding author's e-mail: [basg2004@gmail.com](mailto:basg2004@gmail.com)

### Abstract

Nanobiotechnology is a new era paving a way to develop advanced technology especially in the field of medicine. In the present work, magnetic nanobiocomposite of fungal asparaginase was produced using polyethylene glycol. The formation of magnetic nanobiocomposite of asparaginase was confirmed by laser light scattering and confirmed using UV-Visible spectrophotometer. The specific activity of fungal asparaginase was increased from 320 U/mg of crude asparaginase to 385.81 U/mg of magnetic nanobiocomposite. The primary amines majorly involved in binding of asparaginase on magnetic nanoparticles were confirmed using FT-IR analysis. The AFM analysis has revealed the size of magnetic nanobiocomposite in the range of 130 to 160 nm. The synthesized magnetic nanobiocomposite has shown good cytotoxicity on MCF-7 and HT-29 cancer cell lines. Hence synthesized magnetic nanobiocomposite of fungal asparaginase could be used as an active anticancer drug.

**Keywords:** Fungal asparaginase; Nanobiocomposite; Anticancer drug; Cancer cells; Magnetic nanoparticles; Characterization.

### Introduction

Biological molecules bound to metallic nanoparticles paved new directions in medicinal diagnostics, imaging and biomedical applications [1]. Metal nanoparticles exhibit intrinsic optical properties which will enhance the transparency of polymer-particle composites [2]. Drug delivery focuses on maximizing bioavailability both at specific places of disease in the body and over a period of time. It is all about personalizing drug molecules with the help of nanoparticles and delivering drugs with cell precision. A personalized medicine is intended to avoid damage to normal cells, reduce the drug consumption and treatment expenses resulting in an overall societal benefit by reducing the costs to the public health system [3].

The chemotherapeutic agents such as Carboplatin, Paclitaxel, and Doxorubicin are used to treat cancer along with nanoparticles. The gold nanorods loaded, chitosan conjugated and pluronic based nanocarriers were used as imaging agents for cancer cells and as hyperthermic agents for photothermal cancer therapy. Positive results were reported that the tumor developed in the mouse disappeared in six

days proving that nanoparticles are efficient drug carriers [4,5]. Gold coated silica nanoparticles used for rapid tumor destruction with minimal damage to normal cells [6]. Magnetic nanoparticles provide good stability and poses low toxin to the normal cells [7]. The targeted delivery of PEG modified liposome nanoparticles encapsulated with doxorubicin was reported six times efficient than free doxorubicin treatment [8].

L-asparaginase reduces the L-asparagine content available in the blood as well in the surroundings of the cell. Reduction in the L-asparagine content is responsible for the loss in the viability and necrosis of the cancer cells [9, 10]. Fungal asparaginase was reported for lesser side effect than bacterial asparaginase. The fungi *Aspergillus terreus* can be used for synthesis of asparaginase [11]. Better plasma L-asparaginase activity and effective depletion of asparagine in serum and cerebrospinal fluid was reported for PEG modified L-asparaginase. PEG modified L-asparaginase was reported for more activity than native L-asparaginase [12, 13]. Thus L-asparaginase bound on nanoparticles had promising therapeutic potential for cancer treatment [14]. Hence the present work was

focused on polyethylene glycol mediated fabrication of magnetic nanobiocomposite of fungal asparaginase from *Aspergillus terreus*. Anticancer activity of the synthesized magnetic nanobiocomposite of asparaginase was studied against MCF-7 and HT-29 cancer cell lines.

## Materials and methods

### Microorganisms used

The fungus *Aspergillus terreus* MTCC 1782 was obtained from IMTECH Chandigarh, India. *A. terreus* strain was cultivated in Czapek agar slants at 37°C for 4 days and used as inoculum for the synthesis of asparaginase.

### Reagents and cancer cell lines

The chemicals used for the preparation of magnetic nanobiocomposites are as follows: Ferric chloride (FeCl<sub>3</sub>) and Ferrous Sulphate (FeSO<sub>4</sub>) purchased from CHEMSPURE, India were used as metal precursor for synthesis of magnetic nanoparticles. The binding agent polyethylene glycol and the agar used in Czapek-Dox media were purchased from HIMEDIA Pvt. Ltd., Mumbai, India. The amino acid asparagine was obtained from LOBA CHEMIE Pvt. Ltd., Mumbai and proline was purchased from QUALIGENS, Mumbai, India. The other laboratory reagents used are sourced from SISCO RESEARCH LABORATORIES Pvt. Ltd., Mumbai, India. For the in-vitro analysis, MCF-7 and HT-29 cell lines were obtained from Veterinary College, Vepery, Chennai. The cells were maintained in Minimal Essential Medium supplemented with 10% FBS, penicillin (100 U/ml), and streptomycin (100 µg/ml) in a humidified atmosphere of 50 µg/ml CO<sub>2</sub> at 37°C.

### Preparation of inoculum culture

*Aspergillus terreus* obtained from IMTECH, Chandigarh, India strain was cultivated in Czapek agar slants at 37°C for 4 days.

### Production of asparaginase

*Aspergillus terreus* is inoculated in a 500 ml Erlenmeyer flask containing 200 ml of modified Czapek-Dox liquid medium containing (g/100): 2.0 L-Proline, 1.0 L-Asparagine, 0.2 glucose, 1.0 sodium nitrate, 0.052 potassium chloride, 0.152 Di-potassium hydrogen phosphate, 0.001 zinc sulphate, 0.001 copper sulphate, 0.001 ferrous sulphate and 0.052 magnesium sulphate, maintained at pH 6.2. Then

the fungus was grown aerobically by agitating in an orbital shaker at 160 rpm at 32°C for 4 days [15]. The fermentation broth was filtered under vacuum through Whatman #2 filter paper which is rich with L-asparaginase.

### Chemical synthesis of magnetic nanoparticles

The magnetic nanoparticles were prepared by co-precipitation method. Typically a mixture of solution containing 0.2 M Ferric chloride and 0.1 M Ferrous sulphate are prepared in the presence of a reducing agent (10% NaOH) under constant stirring for magnetic nanoparticle production [16]. The obtained black precipitate was washed with milliQ water and collected by magnetic decantation.

### Pretreatment of magnetic nanoparticle with polyethylene glycol and synthesis of magnetic nanobiocomposite of asparaginase

The black precipitate of magnetic nanoparticle was washed twice with deionized water and then dispersed in 100 mM of PEG4000. The pH of the solution was maintained at 8.5 to enable the attachment PEG4000 to magnetic nanoparticle. The mixture was ultrasonicated for 3 h for well dispersion of PEG pretreated magnetic nanoparticles. Then the mixture was left at room temperature. 100 ml of PEG pretreated magnetic nanoparticle solution was mixed with 50 ml of crude asparaginase for 30 min at 30°C. Then it was kept at 4°C for 6 h and centrifuged at 4°C and 10000 rpm to separate the magnetic nanobiocomposite of asparaginase for further characterization.

### Lyophilization of magnetic nanobiocomposite of asparaginase

The magnetic nanobiocomposite of asparaginase were freeze dried for further characterization. The magnetic nanobiocomposite slurry was taken in 1.5 ml centrifuge vials and centrifuged at 10000 rpm for 10 min. The supernatant were discarded and the pellet was frozen overnight in the freeze drier. The frozen pellets were placed in a freeze dryer chamber and deep frozen to -40°C. The vacuum pump was switched on, so as to reduce the pressure of the drying chamber. Lyophilization was carried out for 4 h. The freeze dried magnetic nanobiocomposite of asparaginase were later stored in the freezer at 4°C for further characterization.

### **Estimation of L-asparaginase activity and protein concentration**

L-Asparaginase activity of crude asparaginase was estimated using Nessler's method. The 0.1 ml of crude asparaginase was mixed with 0.9 ml of 0.1 M phosphate buffer and 1 ml of 0.04 M of L-Asparagine. This mixture was incubated at 37°C for 10 min. The reaction was stopped by adding 0.5 ml of 15% Trichloroacetic acid, after this thorough mixing, it was centrifuged at 6000 rpm for 10 min at 4°C. Then 0.1 ml of supernatant was taken in a separate tube, made up to 8 ml and mixed with this 1 ml of 2 M NaOH and 1ml of Nessler's reagent. Then the mixture was incubated for 10 min at room temperature. Finally absorbance was noted at 480 nm in spectrometer [17]. Protein concentration in crude asparaginase was estimated Bradford method. Sample consisting of 20 µl was mixed with 180 µl of distilled water along with 2 ml of Bradford's reagent separately. This mixture was incubated for 10 min at 37°C in an incubator. Finally absorbance was noted at 595 nm in spectrometer [18].

### **Characterization of synthesized magnetic nanobiocomposites using FTIR, XRD and AFM analysis**

The optical property of the manetic nanobiocomposites was investigated by SYSTRONICS Double Beam UV-Visible spectrophotometer 2201 obtaining spectrum values from 300 to 800 nm. The Fourier Transform Infra-red (FT-IR) spectroscopy was used to analyze the functional groups present in the nanobiocomposites using BRUKER α-T FT-IR Spectrometer. The lyophilized samples were mixed with KBr to form Discs under high pressure using hydraulic press. These discs were scanned from 400 to 4000 cm<sup>-1</sup> to obtain the FT-IR spectra. The details regarding the particle size and surface morphology are observed by Atomic Force Microscope (AFM) (NTMDT, Ireland) analysis. The metallic composition of magnetic nanobiocomposites was analysed using X-ray Diffraction (XRD) spectroscopy.

### **Anticancer activity of magnetic nanobiocomposite of asparaginase against MCF-7 and HT-29 cancer cell lines**

Cancer cells (1×10<sup>5</sup>/well) were plated in 24-well plates and incubated in 37°C with 5% CO<sub>2</sub> condition. After the cell reaches the confluence, the various concentrations of the

samples were added and incubated for 24 h. After incubation, the sample was removed from the well and washed with phosphate-buffered saline (pH 7.4) or MEM without serum. 100 µl/well (5 mg/ml) of 0.5% 3-(4, 5-dimethyl-2-thiazolyl)-2,5-diphenyl-tetrazolium bromide (MTT) was added and incubated for 4 h. After incubation, 1ml of DMSO was added in all the wells. The absorbance at 570 nm was measured with UV-Spectrophotometer using DMSO as the blank [19]. Measurements were performed and the concentration required for a 50% cancer cell inhibition (IC<sub>50</sub>) was determined graphically. The cell viability was calculated using eq. (1).

$$\% \text{ cell viability} = (A_{570} \text{ of treated cells} / A_{570} \text{ of control cells}) \times 100 \dots\dots (1)$$

Graphs are plotted using the % of Cell Viability at Y-axis and concentration of the sample in X-axis. Cell control and sample control is included in each assay to compare the full cell viability assessments.

## **Results and discussions**

### **Asparaginase activity**

The synthesised magnetic nanofluid was black in colour consisting of fine magnetic nanoparticles. The magnetic nanoparticles separated under magnetic field were very fine and black colour in nature (Fig. 1(a)). The intensity of the nanofluid colour was increased to dark brown on the addition of polyethylene glycol (Fig. 1(b)). The specific asparaginase activity was increased from 320 U/mg of crude asparaginase to 385.81 U/mg of asparaginase bound magnetic nanobiocomposite. Thus the presence of asparaginase on the synthesized nanobiocomposite was confirmed. The synthesized nanobiocomposite of asparaginase was found to have good asparaginase activity. Hence it can be used as potential anticancer drug.



Fig. 1. (a) Synthesized magnetic nanoparticles, and (b) L-asparaginase bound magnetic nanoparticles under magnetic field

### UV spectroscopic analysis

The UV absorption spectrum of magnetic nanoparticles (Fig. 2(a)), PEG pretreated magnetic nanoparticles (Fig. 2(b)) and asparaginase magnetic nanobiocomposite colloids (Fig. 2(c)) were observed in the range of 300 to 800 nm. The plasmon peaks in fig. 2 at 477.6 nm confirms the formation of magnetic nanoparticle (Fig. 2(a)) and presence of magnetic nanoparticle in PEG pretreated nanofluid (Fig. 2(b)) and asparaginase magnetic nanobiocomposite (Fig. 2(c)).

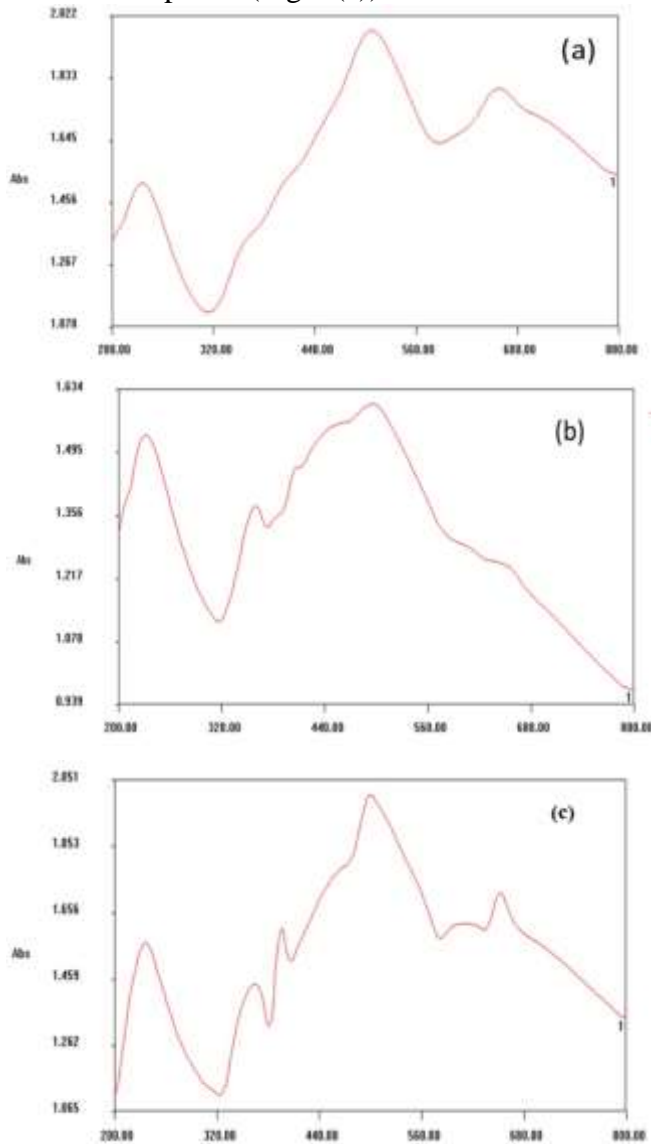


Fig. 2. UV spectrum of (a) Magnetic nanoparticles (b) PEG pretreated magnetic nanoparticles (c) Magnetic nanobiocomposite of asparaginase

### FT-IR analysis of magnetic nanobiocomposite of asparaginase

The interaction between asparaginase and magnetic nanoparticle was analysed by using FT-IR spectroscopy. The spectra represented an

average of 50 scans. All were recorded from 600 to 4000  $\text{cm}^{-1}$  with a resolution of 4  $\text{cm}^{-1}$  as shown in Fig. 3. The pellets of magnetic nanobiocomposite of asparaginase were prepared by gently mixing 1 mg of the lyophilized sample with 100 mg of KBr. There were eight peaks observed as shown in Fig. 3. The peak at 3377  $\text{cm}^{-1}$  confirms the presence of  $-\text{NH}_2$  in aromatic amines, primary amines and amides. The peak at 677  $\text{cm}^{-1}$  represents the presence of strong C-H bond for cis-disubstituted alkenes. The presence of benzene ring confirmed with the peaks at 796, 892 and 1627  $\text{cm}^{-1}$ . The peak at 1066  $\text{cm}^{-1}$  represents the presence of overlapped C-N bond for aliphatic amines. The peak at 1627  $\text{cm}^{-1}$  represents the presence N-O aromatic nitro compounds of conjugated asparaginase on magnetic nanoparticles. Thus the FT-IR results confirmed the presence of bound asparaginase on magnetic nanoparticles.

### XRD analysis of magnetic nanobiocomposite of asparaginase

XRD analysis was used to determine the crystallinity, and metallic nature and cubic structure of magnetic nanoparticles. The lyophilized magnetic nanobiocomposite was subjected for XRD Analysis. Peaks obtained at 30.36 and 43.32  $2\theta$  exhibits the crystalline nature of the synthesized nanobiocomposite (Fig. 4). The peaks in the pattern are highly intensified and very close to each other, this might be caused due to the over agglomeration of the polymer matrix and asparaginase over the magnetic nanoparticle. The masking of the polymer over the magnetic particle produces partiality in the crystalline structure, showing that it is amorphous in state. Generally, an amorphous polymer in an XRD analysis do not show any sharp and extremely intensified peaks whereas the magnetic nanobiocomposite along amorphous polymer (PEG) showed sharp and highly intensified peaks. This is due to the development of crystallinity in the amorphous polymer (Arunkumar et al., 2005).

### Surface morphology and particle size analysis using AFM

The surface morphology such as solid structure, surface area, thickness of synthesized magnetic nanobiocomposite was studied using AFM. The AFM analysis was carried out at 5\*5 and 10\*10 area contact modes. The 2D and 3D surface structures of magnetic nanobiocomposite

observed under 5\*5 area contact mode are shown in as shown in Fig. 5(a) & (b). The histogram analysis provides the size of the magnetic nanobiocomposite. The size of the magnetic nanobiocomposite ranged from 130 to 160 nm.

The magnetic nanobiocomposite was observed with large aggregates, this might be due to the formation of polymer layer and binding of asparaginase enzyme.

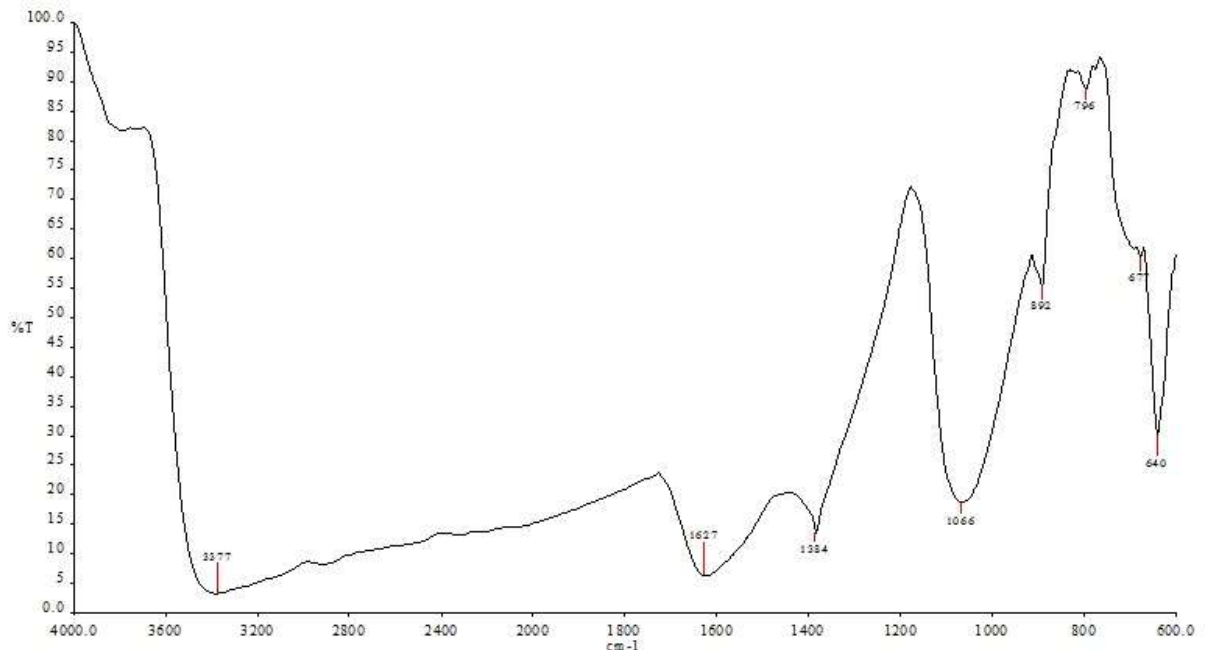


Fig. 3. FT-IR analysis of magnetic nanobiocomposite of asparaginase

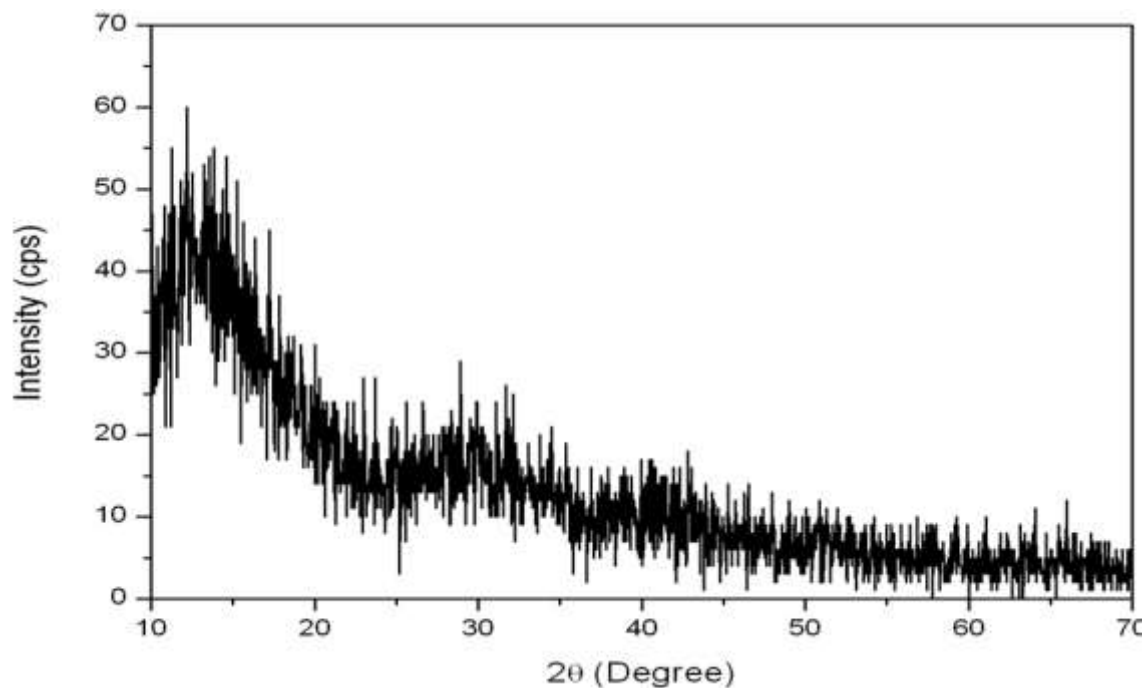


Fig. 4. XRD analysis of magnetic nanobiocomposite of asparaginase

#### **Anticancer activity by MTT assay**

The magnetic nanobiocomposite of asparaginase was tested for its anticancer activity against MCF-7 (Breast cancer) and HT-29 (Human colon adenocarcinoma) cell lines. The concentration of magnetic nanobiocomposite of asparaginase was varied from 1000, 500, 250, 125, 62.5, 31.2, 15.6, and 7.8  $\mu\text{g/ml}$ . The figure 6 shows the anticancer effect of magnetic

nanobiocomposite of asparaginase on HT-29 cell line. The decrease in number of cancer cells was observed corresponding to the increase in magnetic nanobiocomposite of asparaginase concentration. The 1000  $\mu\text{g/ml}$  of magnetic nanobiocomposite of asparaginase showed very few cells while as the 15.6  $\mu\text{g/ml}$  comparatively showed increased number of cells.

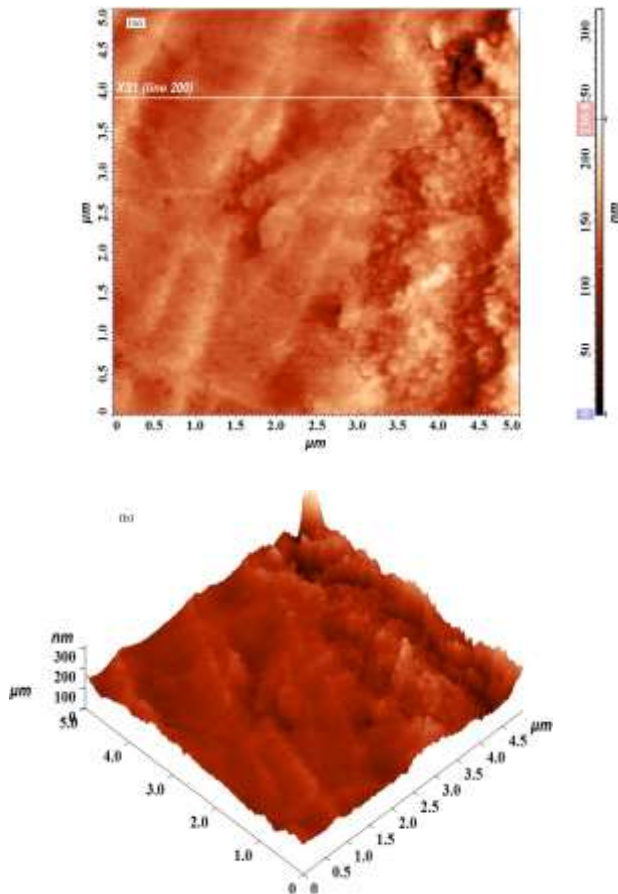


Fig. 5. Surface morphology of magnetic nanobiocomposite of asparaginase (a) 2D and (b)

3D observed under 5\*5 area contact mode

The fig. 7 exhibits the MTT assay of the HT-29 cell line treated with different concentration of magnetic nanobiocomposite of asparaginase. The cell viability was 9.25, 20.37, 29.62, 35.18, 40.74, 44.44, 50 and 55.55 % for 1000, 500, 250, 125, 62.5, 31.2, 15.6 and 7.8  $\mu\text{g/ml}$  of magnetic nanobiocomposite of asparaginase respectively. The cell control had 100% viability. There was a long sustained steady increase in the cell viability on decrease in the concentration of the drug showed steady cytotoxic effect of the drug. The  $\text{IC}_{50}$  value of magnetic nanobiocomposite of asparaginase against HT-29 cell line was found as 125  $\mu\text{g/ml}$ .

The fig. 8 shows the cytotoxic effect magnetic nanobiocomposite of asparaginase againsts MCF-7 cancer cell line. It showed a decrease in growth of MCF-7 cancer cells as the concentration of the magnetic nanobiocomposite of asparaginase increases. The normal MCF-7 cell line was the control used for the in-vitro analysis.

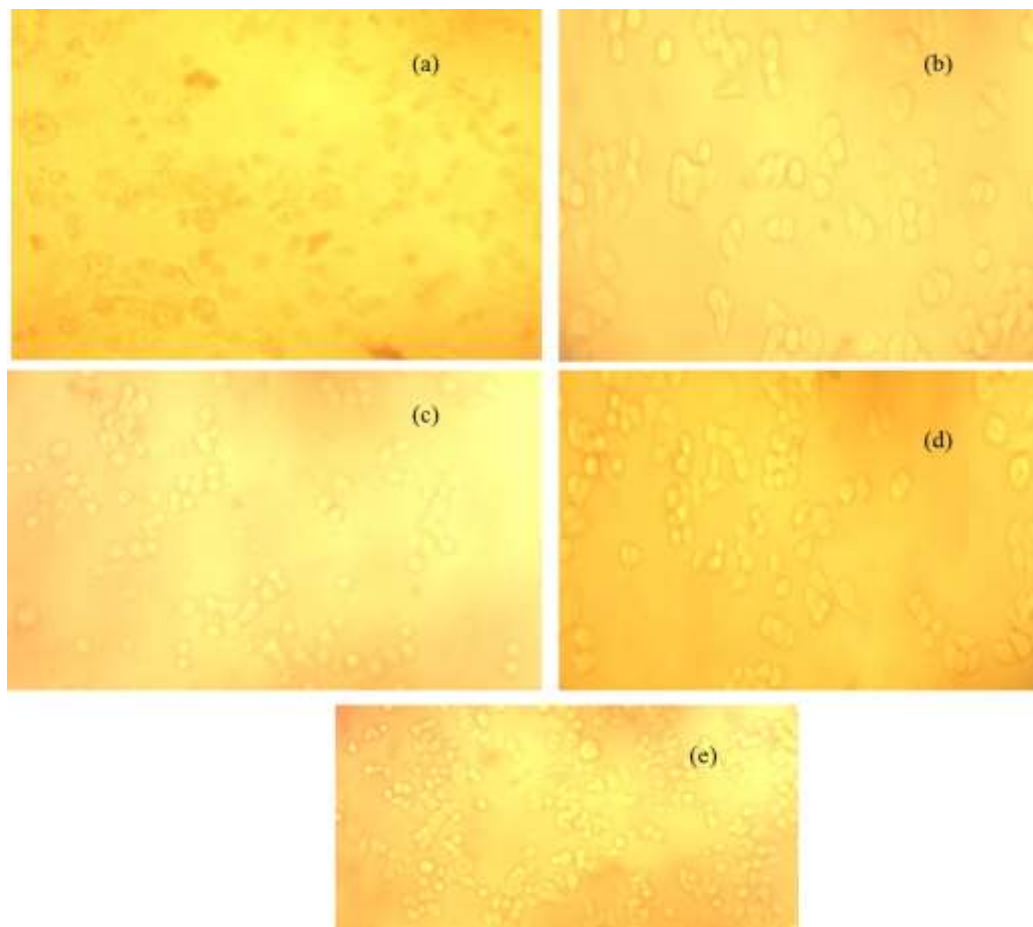


Fig. 6. Cytotoxic effect of magnetic nanobiocomposite of asparaginase on HT-29 cell line (a) 1000  $\mu\text{g/ml}$  (b) 125  $\mu\text{g/ml}$  (c) 62.5  $\mu\text{g/ml}$  (d) 31.2  $\mu\text{g/ml}$  (e) Normal HT-29 Cell line

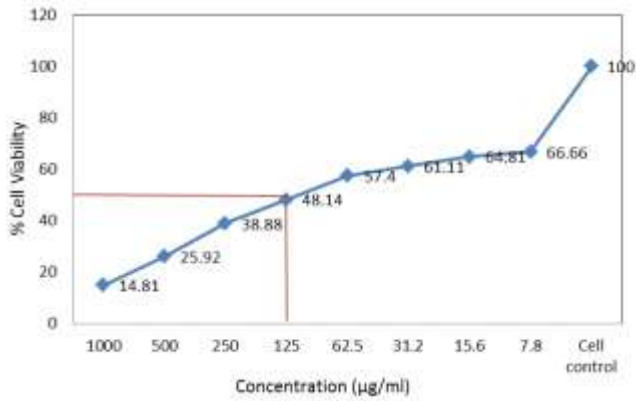


Fig. 7. MTT assay of magnetic nanobiocomposite of asparaginase on HT-29 cell line

The fig. 9 shows the MTT assay of MCF-7 cancer cell lines treated with different concentration of magnetic nanobiocomposite of asparaginase and its anticancer effect. The cell

viability was 10.20, 10.32, 26.53, 40.81, 48.97, 51.10, 59.18 and 63.26% for 1000, 500, 250, 125, 62.5, 31.2, 15.6 and 7.8 µg/ml of magnetic nanobiocomposite of asparaginase respectively. The cell control had 100% cell viability. There was a gradual increase in the cell viability on decrease in the concentration of the drug showed stable cytotoxic effect of the drug. The  $IC_{50}$  value of magnetic nanobiocomposite of asparaginase against MCF-7 cell line was found as 62.5 µg/ml. On comparison of the both cancer cell lines the rapid destruction of the cancer cell were observed on the MCF-7 cancer cell line [20]. Thus the magnetic nanobiocomposite of asparaginase is more effective against MCF-7 cancer cell line than HT-29 cell line.

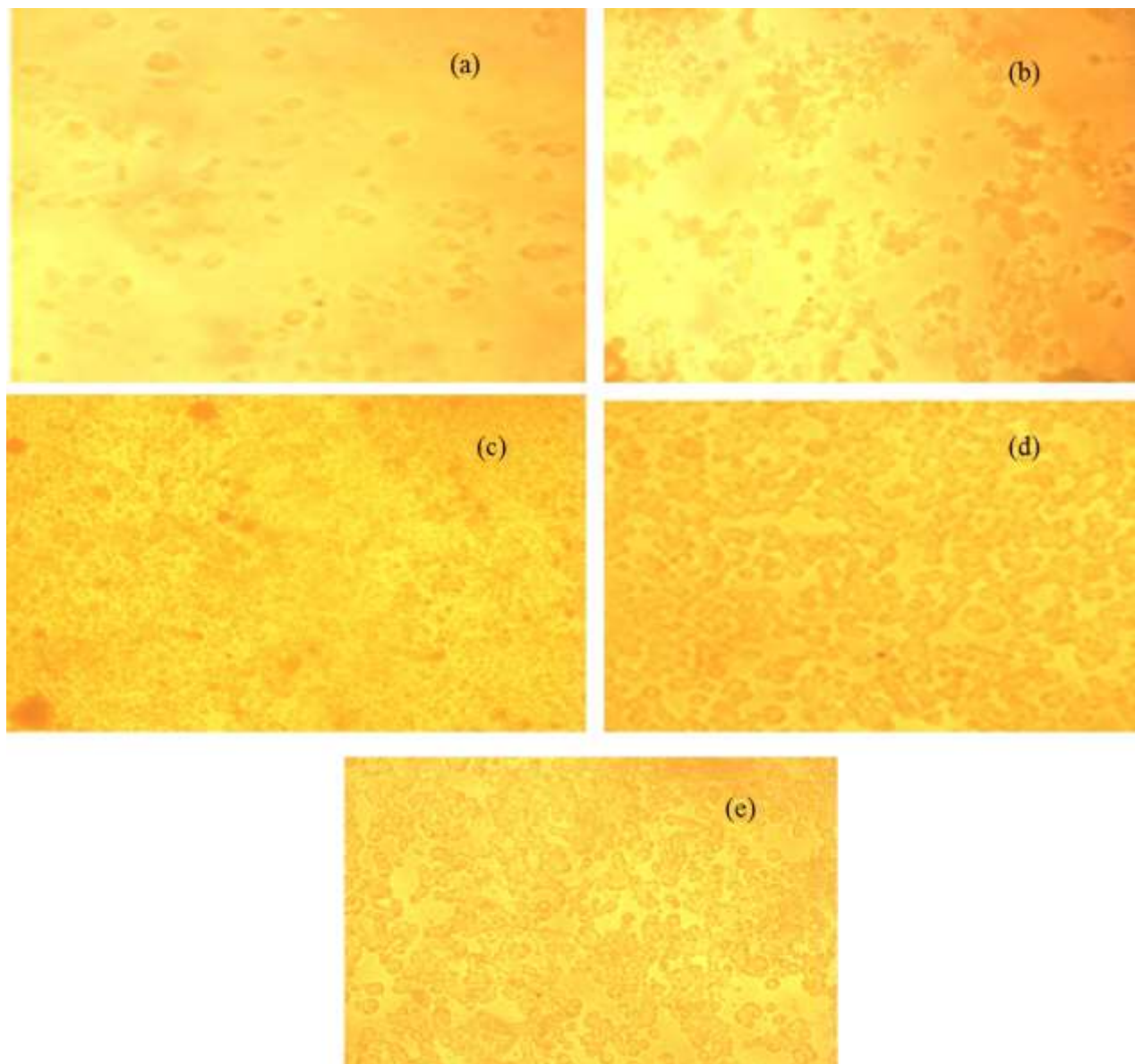


Fig. 8. Cytotoxic effect of magnetic nanobiocomposite of asparaginase on MCF-7 cell line (a) 1000 µg/ml (b) 125 µg/ml (c) 62.5 µg/ml (d) 31.2 µg/ml (e) Normal MCF-7 Cell line

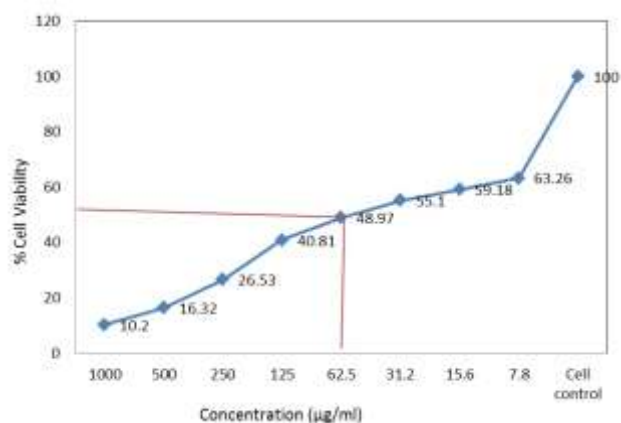


Fig. 9. MTT assay of magnetic nanobiocomposite of asparaginase on MCF-7 cell line

### Conclusions

The fungal asparaginase was effectively immobilized on magnetic iron nanoparticles by using polyethylene glycol. An increase in specific activity of immobilized asparaginase was increased to 385.81 U/mg from 320 U/mg of crude asparaginase. The peaks in the UV spectroscopy indicated the presence of gamma iron oxide. The FT-IR peaks elucidated the functional groups involved in binding of asparaginase. The XRD analysis showed the partial crystallinity of magnetic nanobiocomposite of asparaginase. The AFM analysis showed the average particle size and the surface texture. The steady decrease in viability cancer cells were observed for increases in concentration of magnetic nanobiocomposite of asparaginase. The in-vitro assay displayed the rapid destruction of the cells were observed on the MCF-7 cancer cell line. Thus the magnetic nanobiocomposite of asparaginase is more effective against MCF-7 cancer cell line than HT-29 cell line.

### Conflicts of interest

The authors declare no conflict of interest.

### References

- [1] Shiho T, Yojiro Y, Hiroshi SB, Tsutomu N. Synthesis and bioanalytical applications of specific-shaped metallic nanostructures: A review. *Analytica Chimica Acta* 2012;716:76-91.
- [2] Buzea C, Pacheco II, Kevin R. Nanomaterials and nanoparticles: sources and toxicity. *Biointerphases* 2007;02:MR17-71.
- [3] Freitas Jr AR. What is nanomedicine, Nanomedicine: Nanotechnology, Biology and Medicine 2005;1:2-5.
- [4] Choi CH, Alabi CA, Webster P, Davis ME. Mechanism of active targeting in solid tumors with transferrin-containing gold nanoparticles. *Proc Natl Acad Sci* 2010;107:1235-40.
- [5] Baskar G, Chandhuru J, Fahad KS, Praveen AS, Chamundeeswari M, Muthukumar T. Anticancer activity of fungal L-asparaginase conjugated with zinc oxide nanoparticle. *Journal of Materials Science: Materials in Medicine* 2015;26:43.
- [6] Smith AM, Dave S, Nie S, True L, Gao X. Multicolor quantum dots for molecular diagnostics of cancer. *Expert Rev Mol Diagn* 2006;6:231-44.
- [7] Suphiya P, Ranjita M, Sanjeeb KS. Nanoparticles: A boon to drug delivery, therapeutics, diagnostics and imaging. *Analytica Chimica Acta* 2012;716:7-91.
- [8] Gullotti E, Yeo Y. Extracellularly activated nanocarriers: a new paradigm of tumor targeted drug delivery. *Mol Pharm* 2009;6:1041-51.
- [9] Haley EE, Fisher GA. The requirement of L-asparagine of mouse leukemia cells L5178Y in culture. *Cancer Res* 1961;21:532-36.
- [10] Mitchell I, Hoogendoorn H, Giles AR. Increased endogenous thrombin generation in children with acute lymphoblastic leukemia: risk of thrombotic complications in L-asparaginase induced antithrombin III deficiency. *Blood* 1994;83:386-391.
- [11] Baskar G, Renganathan S. Statistical and evolutionary optimisation of operating conditions for enhanced production of fungal L-asparaginase. *Chemical Pap* 65;2011:798-804
- [12] Hawkins DS, Park JR, Thomson BG, Felgenhauer JL, Holcenberg JS, Panosyan EH, Avramis VI. Asparaginase pharmacokinetics after intensive polyethylene glycol conjugated L-asparaginase therapy for children with relapsed acute lymphoblastic leukemia. *Clinical Cancer Research* 2004;10:5335-41.
- [13] Rizzari C, Citterio M, Zucchetti M, Conter V, Chiesa R, Colombini A, Malguzzi S, Silvestri D, D'Incalci M. A



- pharmacological study on pegylated asparaginase used in front-line treatment of children with acute lymphoblastic leukemia. *Haematologica* 2006;91:24-31.
- [14] Baskar G, Chandhuru J, Praveen AS, Fahad KS. Anticancer activity of iron oxide nanobiocomposite of fungal asparaginase. *International Journal of Modern Science and Technology* 2017;2:98-104.
- [15] Baskar G, Renganathan S. Optimization of L-asparaginase production by *Aspergillus terreus* MTCC 1782 using response surface methodology and artificial neural network linked genetic algorithm. *Asia-Pac J Chem Eng* 2012;7:212-20.
- [16] Shen YF, Tang J, Nie ZH, Wang YD, Ren Y, Zuo L. Preparation and application of magnetic Fe<sub>3</sub>O<sub>4</sub> nanoparticles for wastewater purification. *Sep Purif Technol* 2009;68:312-319.
- [17] Wriston Jr JC, Yellin TO. L-asparaginase: A review. *Adv Enzymol Relat Areas Mol Biol* 1973;39:185-248.
- [18] Bradford M. A rapid and sensitive method method for the quantification of microgram quantities of protein utilizing the principle of protein-dye binding. *Anal Biochem* 1974;72: 248-54.
- [19] Mosmann T. Rapid colorimetric assay for cellular growth and survival: Application to proliferation and cytotoxicity assays. *J Immunol Methods* 1983;65:55-63.
- [20] Baskar G, George GB. Glutaraldehyde-Mediated Synthesis of Asparaginase-Bound Maghemite Nanocomposites: Cytotoxicity against Human Colon Adenocarcinoma Cells. *Asian Pac J Cancer Prev* 2016;17:4237-40.

\*\*\*\*\*